Finite Element Analysis of Delaminated Composite Plate Under Bending

Dr. Najeeb .A. Yahya, Nureddin.O.Fahel Alboum and Othman.M.Daas
Dept. of Mechanical and Industrial Engineering, Faculty of Engineering,
Zawia University

Abstract:

This paper describes the delamination analysis of simply supported composite laminate plate in bending. The theoretical formulation is based on three plate model. The finite element method is used to analyse the laminate plate delamination, which is based on the theory of Midline plate and the eight-node isoparameter laminated plate element. The computer program for the determination of deformation and stress fields of composite laminate used to calculate the deflection at plate centre. The study includes the plate with and without delamination when effect by

lamination angle, delamination area ratio and the location of the delamination along the thickness. Tsai-Hill criterion, Tsai-Wu criterion and Hoffman criterion are used to check the failure of the composite laminate. To investigate the first ply failure load, parametric studies are made for different cases by varying the size delamination as well as the stacking sequences. The results are presented in a tabular and graphical form showing the delamination area is directly proportional to the deflection at plate centre and the deflections of delamination plate are larger than deflections of perfect plate.

Key words: *Finite element analysis, composite material, bending load, three plate model, delamination.*

1. Introduction:

Laminated composites are materials widely used for replacing metals in many engineering structures, such as aerospace, automobile, nuclear, marine, biomedical, and sports equipment due to their high specific stiffness, high strength, and low weight [1]. Even though widely utilized, the potential and behavior of laminated composites are not fully exploited [2, 3, 4, 5]. Thus, further investigation are required, especially related to failure mechanisms of composite laminates. Delamination is one of the most common failure modes that may occur between laminas subjected to transverse loading. Delamination occurs when the bonds between layers of the laminate fail due to debonding in the plane of the interface adhesion [6]. The existence of delamination can reduce the strength, stiffness, and load-bearing capacity of the laminate under compressive loads [7]. Extensive research has been carried out on the

delamination mechanism of composite laminates [8, 9, 10, 11, 12]. Detecting this type of damage is still a serious problem in composite structures.

The presence of delamination in a laminated composite material may reduce the overall stiffness and causes structural degradation, stiffness reduction and failure at stress well below the strength levels expected for defect free material. Since interlaminar strength is very low and interlaminar stresses are usually high. The analysis of delamination of laminated composite plate becomes quite attractive to engineers. There are some approaches to solve that problem. Kameran et al. [13] presented the behavior of laminated composite plates under transverse loading using an eight-node isoparameter quadratic element based on first order shear deformation theory, the element has six degrees of freedom at each node: translations in the nodal x , y and z directions and rotations about the nodal x , y and z axes. Cochelin et. al. [14] suggested the 'three-plate model' and used it to investigate the buckling of delaminated plates. Chen [15] use the shear deformation theory to find compressive delamination buckling and growth of buckling. The geometry of delamination buckling is based on three-plate model. The results of various length ratios and thickness ratios of delamination vs. plate are calculated.

In this paper the similar model is selected to describe the delamination of laminated plates. The eight-node isoparameter laminated plate element is used, which is based on the theory of Midline Plate. The results for laminated plates in bending are presented.

2. Mechanical properties of the material and ultimate strength:

Table 1 shows the properties of graphite/epoxy composites material used in this study. The properties are obtained from the relevant manufacturers and literature data [16].

Table 1 Materials properties of graphite/epoxy composites

Material type	Young's Modulus (GPa)		Shear Modulus (GPa)		Poisson's ratio
Graphite/epoxy composite	E_{11}	E_{22}	G_{12}	G_{23}	$\nu_{12} = \nu_{23}$
	126.0	8.0	3.7	2.7	0.26

Ultimate strength;

$X_t = 1415\ MPa$ $X_c = 1232\ MPa$ $Y_t = 35\ MPa$

$Y_c = 157\ MPa$ $S_{12} = 63.9\ MPa$ $S_{23} = 50\ MPa$

where: ‘‘*X*” and ‘‘*Y*” denote the strength along the fibre direction and transverse to it, respectively; the subscripts ‘‘t” and ‘‘c” signify the tensile and compressive strengths. And ‘‘*S*” denote the shear strengths of a lamina in 12 and 23 planes, respectively.

3. Geometry of the delamination plate:

The geometry of the delaminated plate is shown in Figure 1. This model contains the circle delamination with the radius R_d located arbitrarily through the thickness at plate center.

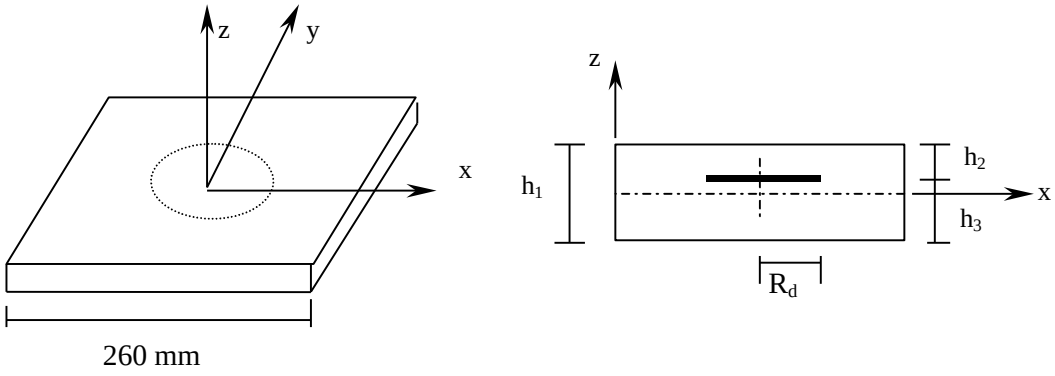

Figure 1 Geometry of the delaminate laminate plate

The thickness of plate is depending on the number of layers and the thickness of each layer. The location of delamination is obtained by the h_3/h_1ratio where the thickness of upper sublaminate and the lower sublaminate are h_2 and h_3 respectively.

In this paper four-group graphite/epoxy specimen of composite laminate plates with size (260×260×2.25) are selected for the analyses. The first group specimen is perfect plate while the left groups specimens are delaminated composite laminate plates, where the delamination areas of each specimen are different. The specimen specifications are shown in Table 2. Each group contains four specimens and each specimen has two types of the composite laminate with fabric orientations are used. The first type is angle ply antisymmetric eighteen layers $[\theta,-\theta]_9$ and the second type is nine layers cross-ply $[[0^o,90^o]_2,0^o,[90^o,0^o]_2]$ symmetric laminate.

Table 2 Specimen specifications

	Delamination Radius R_d (mm)	Delamination area to plate area ratio A_d/A
Group-1	0.0	0.0
Group -2	41.0	0.078
Group -3	53.5	0.133
Group -4	63.0	0.184

4. Finite element model and formulation:

The element used is the eight-node quadrilateral laminated element. The element has forty degrees of freedom, three translational displacements and two rotations at each node. The formulation of eight-node isoparametric finite laminated is derived. The configuration of element is shown in Figure 2. The coordinate and displacement in the isoparametric

$$x=\sum_{i=1}^{8}N_i x_i \qquad y=\sum_{i=1}^{8}N_i y_i \qquad z=\sum_{i=1}^{8}N_i \frac{t_i}{2}\zeta$$
$$u_0=\sum_{i=1}^{8}N_i u_i \qquad v_0=\sum_{i=1}^{8}N_i v_i \qquad w_0=\sum_{i=1}^{8}N_i w_i \qquad (1)$$

element can be written as;

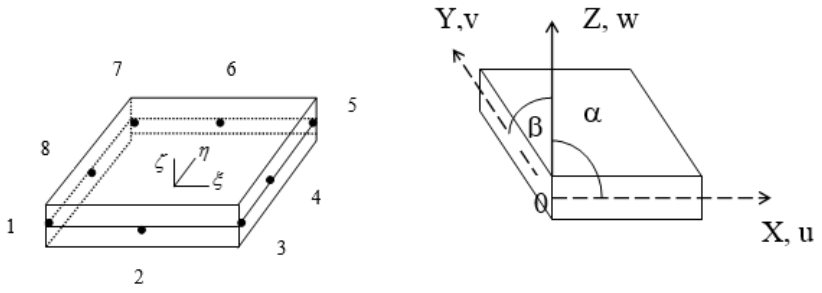

Figure 2 Isoparametric plate element

where: x , y and z are the coordinates at any point of element. x_i , y_i and z_i are the nodal coordinates. N_i is the interpolation function, t_i is the thickness of element. u_0 , v_0 and w_0 the middle-plane displacements, u_i , v_i and w_i the nodal displacement in x , y and z directions respectively.

The displacement field is written as:

$$u = u_0 + z\alpha = \sum_{i=1}^{8} N_i u_i + \sum_{i=1}^{8} N_i \frac{t_i}{2}\zeta\alpha_i$$
$$v = v_0 + z\beta = \sum_{i=1}^{8} N_i v_i + \sum_{i=1}^{8} N_i \frac{t_i}{2}\zeta\beta_i \quad (2)$$
$$w = \sum_{i=1}^{8} N_i w_i$$

The nodal displacement vector at node k is δ_k

$$\delta_k = \begin{bmatrix} u & v & w & \alpha & \beta \end{bmatrix}_k^T \qquad k = (1,2,\ldots,8) \quad (3)$$

The strain vector at node k is

$$\varepsilon_k = \begin{bmatrix} \varepsilon_x & \varepsilon_y & \gamma_{xy} & \gamma_{xz} & \gamma_{yz} \end{bmatrix}_k^T \quad (4)$$

$$\{\varepsilon\}_k = [B]_k \{\delta\}_k \quad (5)$$

where the $[B]_k$ is the strain displacement transformation matrix can be form as:

$$[B]_k = \begin{bmatrix} \frac{\partial N_i}{\partial x} & 0 & 0 & \frac{1}{2}\frac{\partial N_i}{\partial x} t_i \zeta & 0 \\ 0 & \frac{\partial N_i}{\partial y} & 0 & 0 & \frac{1}{2}\frac{\partial N_i}{\partial y} t_i \zeta \\ \frac{\partial N_i}{\partial y} & \frac{\partial N_i}{\partial x} & 0 & \frac{1}{2}\frac{\partial N_i}{\partial y} t_i \zeta & \frac{1}{2}\frac{\partial N_i}{\partial x} t_i \zeta \\ 0 & 0 & \frac{\partial N_i}{\partial x} & \frac{1}{2} N_i t_i \frac{\partial \zeta}{\partial z} & 0 \\ 0 & 0 & \frac{\partial N_i}{\partial y} & 0 & \frac{1}{2} N_i t_i \frac{\partial \zeta}{\partial z} \end{bmatrix} \quad (6)$$

The general form for eight-node isoparametric plate element the strain-displacement matrix can be written as.

$$B = [B_1 \quad B_2 \quad B_3 \quad \dots \quad B_8] \quad (7)$$

Stress-strain relation

$$\{\varepsilon\} = [S]\{\sigma\} \quad (8)$$

where $[S]$ is the compliance matrix, and stiffness matrix $[C] = [S]^{-1}$

The stress and strain transformation from material axes 1, 2 and 3 to the reference axes x, y and z by trigonometric functions of the angle rotation.

$$\{\varepsilon_x\} = [T]^T \{\varepsilon_1\} \qquad \{\sigma_x\} = [T]^{-1} \{\sigma_1\} \quad (9)$$

and the transformed stiffness matrix is

$$\left[\bar{C}\right] = [T][C][T]^T \quad (10)$$

The equation can be written as:

$$\{\sigma\}_{xyz} = \left[\bar{C}\right]\{\varepsilon\}_{xyz} \tag{11}$$

$$\left[\bar{C}\right] = \begin{bmatrix} \bar{C}_{11} & \bar{C}_{12} & \bar{C}_{13} & \bar{C}_{14} & 0 & 0 \\ \bar{C}_{21} & \bar{C}_{22} & \bar{C}_{23} & \bar{C}_{24} & 0 & 0 \\ \bar{C}_{31} & \bar{C}_{32} & \bar{C}_{33} & \bar{C}_{34} & 0 & 0 \\ \bar{C}_{41} & \bar{C}_{42} & \bar{C}_{43} & \bar{C}_{44} & 0 & 0 \\ 0 & 0 & 0 & 0 & \bar{C}_{55} & \bar{C}_{56} \\ 0 & 0 & 0 & 0 & \bar{C}_{65} & \bar{C}_{66} \end{bmatrix} \tag{12}$$

For a thin walled structure of composite material the condition is usually considered.

$$\sigma_z = 0$$

The stiffness matrix of material can be reduce from 6×6 to 5×5 as follows:

$$[D] = \begin{bmatrix} D_{11} & D_{12} & D_{13} & 0 & 0 \\ D_{21} & D_{22} & D_{23} & 0 & 0 \\ D_{31} & D_{32} & D_{33} & 0 & 0 \\ 0 & 0 & 0 & D_{44} & D_{45} \\ 0 & 0 & 0 & D_{54} & D_{55} \end{bmatrix} \tag{13}$$

The element stiffness matrix K can be written as

$$[K] = \int_{-1}^{1}\int_{-1}^{1}\int_{-1}^{1} [B]^T [D][B]|J|d\xi\, d\eta\, d\zeta \qquad (14)$$

$$= \sum_{i=1}^{n} \int_{-1}^{1}\int_{-1}^{1}\int_{-1}^{1} [B]^T [D][B]|J|\frac{h_k}{t} d\xi\, d\eta\, d\zeta_k$$

where D is the stiffness matrix of material, $|J|$ is the Jacobean determinate and h_k is the thickness of the k[th] layer.

4.1. Three-plate model:

In this model the composite laminated plate is considered. This plate contains a single delamination of arbitrary shape, which separates two sets of plies of respective thickness h_2 and h_3. The thickness of the original plate is h_1. The geometry of the model is shown in Figure 3.

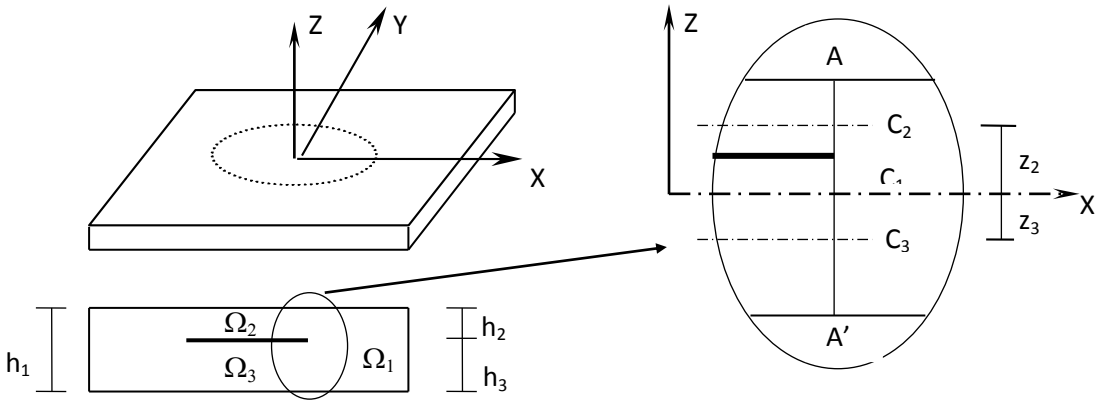

Figure 3 Delaminated laminate

Because of the symmetry of the model, only half of the plate is considered and is divided into three segments referred separately as base plate (Ω_1), upper sub-laminate (Ω_2), and lower sub-laminate (Ω_3). These three plates are considered as three Midline plates. The nodes of those plates are at middle-plane of respective plates shown in Figure 3. Assume that $\delta^{(1)}$,$\delta^{(2)}$ and $\delta^{(3)}$ represent the nodal displacement vectors of plates Ω_1,Ω_2 and Ω_3, respectively.

$$\delta^{(1)}=[u^{(1)}, v^{(1)}, w^{(1)}, \alpha^{(1)}, \beta^{(1)}]$$
$$\delta^{(2)}=[u^{(2)}, v^{(2)}, w^{(2)}, \alpha^{(2)}, \beta^{(2)}] \quad (15)$$
$$\delta^{(3)}=[u^{(3)}, v^{(3)}, w^{(3)}, \alpha^{(3)}, \beta^{(3)}]$$

where $u^{(i)}$, $v^{(i)}$ and $w^{(i)}$ (i = 1,2,3) are displacement components of nodes, and $\alpha^{(i)}$, $\beta^{(i)}$ (i = 1,2,3) are the angles of rotation of the normal to the middle surfaces for plates Ω_1 ,Ω_2 and Ω_3 , respectively. The conditions of compatibility for the displacements in the frontier of delamination of the 'three-plate model' can be expressed as follows:

$$\alpha^{(1)} = \alpha^{(2)} = \alpha^{(3)} \quad ; \quad \beta^{(1)} = \beta^{(2)} = \beta^{(3)} \quad ; \quad w_{c1} = w_{c2} = w_{c3} \quad (16)$$

$$u_{c2}^{(2)} = u_c^{(1)} = z_2\alpha^{(2)} \quad ; \quad v_{c2}^{(2)} = v_c^{(1)} = z_2\beta^{(2)}$$
$$u_{c3}^{(3)} = u_c^{(1)} = z_3\alpha^{(3)} \quad ; \quad v_{c3}^{(3)} = v_c^{(1)} = z_3\beta^{(3)} \quad (17)$$

The relationship of the nodal displacement vector of above three plates can be expressed by means of the transform matrices as follows:

$$\delta^{(2)}=\mathbf{T}_2\,\delta^{(1)} \qquad \delta^{(3)}=\mathbf{T}_3\,\delta^{(1)} \quad (18)$$

where $[T_2]=\begin{bmatrix}1&0&0&z_2&0\\0&1&0&0&z_2\\0&0&1&0&0\\0&0&0&1&0\\0&0&0&0&1\end{bmatrix}$; $[T_3]=\begin{bmatrix}1&0&0&z_3&0\\0&1&0&0&z_3\\0&0&1&0&0\\0&0&0&1&0\\0&0&0&0&1\end{bmatrix}$ (19)

The corresponding element stiffness matrix can be written as:

$$\mathbf{K}_{(i)}^{e} = \sum_{k=1}^{n} \int_{-1}^{1}\int_{-1}^{1}\int_{-1}^{1} \mathbf{T_i}^{T}\mathbf{B}^{T}\mathbf{D}\mathbf{B}\mathbf{T_i}|\mathbf{J}|\frac{h_k}{t} d\xi d\eta d\zeta_k \qquad (20)$$

4.2. Failure criteria

A failure theory is required to assess whether the composite ply has failed or not under an applied stress system. The interactive criteria have been investigated, extending to the case of orthotropic materials.

Tsai-Hill criteria:

Index failure.

$$F = \left(\frac{\sigma_1}{X}\right)^2 + \left(\frac{\sigma_2}{Y}\right)^2 - \left(\frac{\sigma_1}{X}\right)\left(\frac{\sigma_2}{X}\right) + \left(\frac{\tau_{23}}{S_{23}}\right)^2 + \left(\frac{\tau_{31}}{S_{31}}\right)^2 + \left(\frac{\tau_{12}}{S_{12}}\right)^2$$

Load factor

$$R = \frac{1}{\sqrt{F}}$$

where the $(\sigma_1, \sigma_2, \tau_{12}, \tau_{23}, \tau_{31})$ are the stress and (S_{12}, S_{23}, S_{31}) are the shear strength components referred to the lamina coordinate axes (1,2,3). The appropriate values of $(X_t \; or \; X_c \; and \; Y_t \; or \; Y_c)$ must be used depending on the signs of $\sigma_1 \; and \; \sigma_2$.

Hoffman criteria:

Index failure.

$$F = \frac{\sigma_1^2}{X_t X_c} + \frac{\sigma_2^2}{Y_t Y_c} - \frac{\sigma_1 \sigma_2}{X_t X_c} + \left(\frac{X_c - X_t}{X_t X_c}\right)\sigma_1 + \left(\frac{Y_c - Y_t}{Y_t Y_c}\right)\sigma_2 + \left(\frac{\tau_{23}}{S_{23}}\right)^2 + \left(\frac{\tau_{31}}{S_{31}}\right)^2 + \left(\frac{\tau_{12}}{S_{12}}\right)^2$$

Load factor $AR + BR^2 - 1 = 0$

$$R1, R2 = \frac{-B \pm \sqrt{B^2 + 4AC}}{2A}$$

where

$$A = \frac{\sigma_1^2}{X_t X_c} + \frac{\sigma_2^2}{Y_t Y_c} - \frac{\sigma_1 \sigma_2}{X_t X_c} + \left(\frac{\tau_{23}}{S_{23}}\right)^2 + \left(\frac{\tau_{31}}{S_{31}}\right)^2 + \left(\frac{\tau_{12}}{S_{12}}\right)^2$$

Tsai-Wu criteria:

$$B = \left(\frac{X_c - X_t}{X_t X_c}\right)\sigma_1 + \left(\frac{Y_c - Y_t}{Y_t Y_c}\right)\sigma_2$$

Index failure.

$$F = \frac{\sigma_1^2}{X_t X_c} + \frac{\sigma_2^2}{Y_t Y_c} - \frac{\sigma_1 \sigma_2}{\sqrt{X_t X_c Y_t Y_c}} + \left(\frac{X_c - X_t}{X_t X_c}\right)\sigma_1 + \left(\frac{Y_c - Y_t}{Y_t Y_c}\right)\sigma_2 + \left(\frac{\tau_{23}}{S_{23}}\right)^2 + \left(\frac{\tau_{31}}{S_{31}}\right)^2 + \left(\frac{\tau_{12}}{S_{12}}\right)^2$$

Load factor $AR + BR^2 - 1 = 0$

$$R1, R2 = \frac{-B \pm \sqrt{B^2 + 4AC}}{2A}$$

where

$$A = \frac{\sigma_1^2}{X_t X_c} + \frac{\sigma_2^2}{Y_t Y_c} - \frac{\sigma_1 \sigma_2}{\sqrt{X_t X_c Y_t Y_c}} + \left(\frac{\tau_{23}}{S_{23}}\right)^2 + \left(\frac{\tau_{31}}{S_{31}}\right)^2 + \left(\frac{\tau_{12}}{S_{12}}\right)^2$$

$$B = \left(\frac{X_c - X_t}{X_t X_c}\right)\sigma_1 + \left(\frac{Y_c - Y_t}{Y_t Y_c}\right)\sigma_2$$

5. Results and Discussion:

5.1. Validation:

The formulation of finite element method was implemented in the computer program for the determination of deflection of square composite laminate plate. Suppose that perfect laminated composite plate is subjected to uniform distribution load (q_o). The boundary condition is simply supported which is a three-layer cross-ply $[0^o, 90^o, 0^o]$.The geometry is shown in Figure 4a. The layers have equal thickness. The properties of graphite/epoxy composites material used are the same as in Table 1. Computer codes are developed based on present finite element method. The numerical results obtained are compared and validated with the results of published literatures [17, 18] as furnished in Table 3. The numerical results show an excellent agreement with the previously published results and hence it demonstrates the capability of the computer codes developed and proves the accuracy of the analyses.

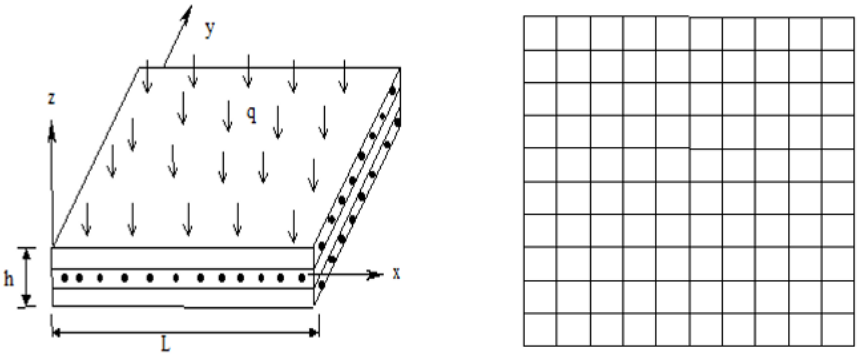

Figure 4 (a) Geometry of cross ply $[0^o, 90^o, 0^o]$ square plate, (b) Mesh type for FEM

The mesh size (10 x 10) consisting of 100 elements and 341 nodes, has been used for the analysis due to computational efficiency. The total number of degrees of freedom involved in the computation is 1705 as each node of the isoparametric plate bending element is having five degrees of freedom comprising of three translations and two rotations. The finite element results obtained when the mesh for the composite plate is shown in Figure 4b. Table 3 shows the effect of length to thickness ratio (L/h) on the non-dimensional deflection at plate centre, which is represented by dimensionless quantity $\bar{w}_c$.

The non-dimensional centre deflection is:

$$\overline{Wc} = W_C * \frac{E_2 h^3}{q_o L^4} * 10^2$$

Table 3 Results for a three-layer cross-ply [0^o, 90^o, 0^o] square plate

L/h	Non-dimensional deflection ($\bar{w}_c$)		
	A simple higher-order theory for laminate composite plate Ref [17]	Analysis of delaminated composite plate by FEM with fine mesh Ref [18]	Present (FEM)
10	1.0900	1.0832	0.9800
20	0.7760	0.7742	0.7510
50	0.6838	0.6592	0.6810
100	0.6705	0.5851	0.6750

In addition, another mesh for the laminated composite plate is considered for model verification. This mesh is shown in Figure 5. The results are compared with the numerical work by Reddy [17]. It is obvious that the present model demonstrates are in better agreement with the

numerical results by Xuanling [18]. From Table 3 when the ratio L/h ≥ 20 the FEM results are closer to the results obtained based on the high-order theory solution ref [17].

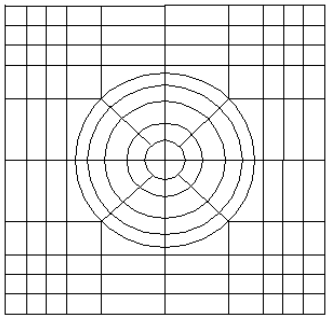

Figure 5 Mesh type for FEM analysis

5.2. The effect of the lamination angle on the deflection at the plate centre:

The deflection at the centre of composite plate was determined for the square plate without delamination and with circle delamination. The material properties used are the same as in Table 1. The angle ply antisymmetric eighteen layers $[\theta, -\theta]_9$ plate are selected where the delamination area to plate area ratio $A_d/A = 0.078$, and the thickness ratio $h_3/h_1 = 0.8333$. The plate is subjected to uniform distribution load q is equal to 2×10^{-3} N/mm^2. Boundary conditions are simply supported. Figure 6 is shows that the deflection at the plate center (w_c) in function of the layer angle (θ). The curves are symmetric about the line at angle 45^o. The results show that, the maximum value of deflection is for angles 0^o and 90^o of 13 mm and the minimum value is 7.7 mm for angle 45^o. The deflections of

delamination plate are larger than deflections of perfect plate. Figure 6 is similar to the figure in the Ref [18].The orientation of fibre has significant effect on the deflection at the plate centre.

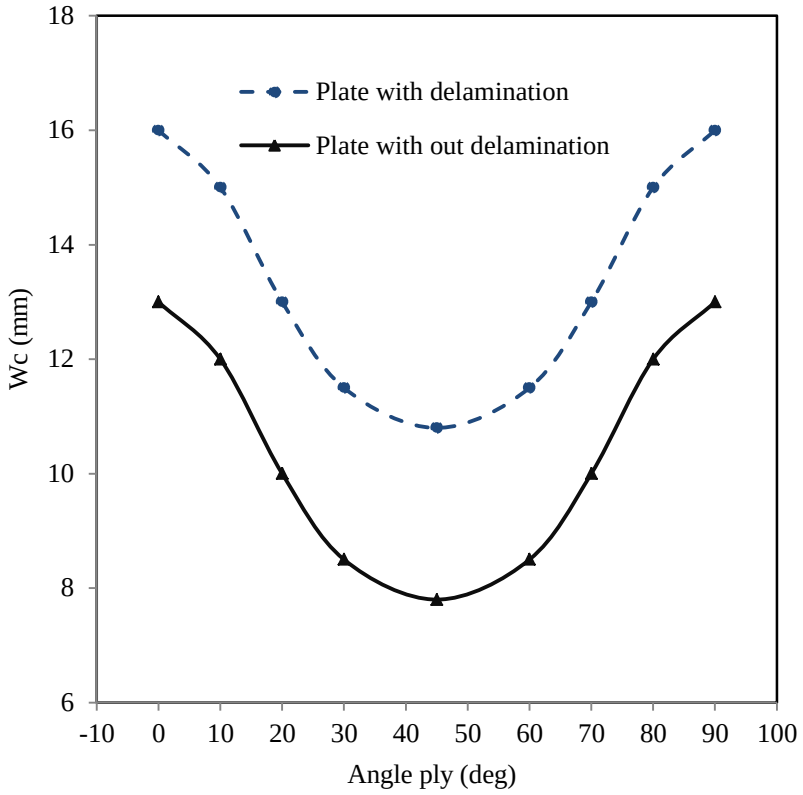

Figure 6 Deflection versus angle ply, A_d/A = 0.078

5.3. The effect of the location of delamination along the thickness of plate on the deflection at the plate centre:

The quantity h_3/h_1 ratio according to Figure 1 represents the location of delamination along the thickness of the plate. The large value of this ratio indicates a near surface delamination. For example, angle ply anti-symmetric eighteen layers $[\theta, -\theta]_9$, the material properties used are the same as in Table 1 where the angles ply $\theta = 30^o, 45^o$. The delamination area ratio is constant $A_d/A = 0.078$. The relationship between the deflection (W_C) and the h_3/h_1 ratio is plotted in in Figure 7. Table 4 lists the h_3/h_1 ratio for the plate with delamination of different angles ply.

Table 4 Relationship between h_3/h_1 ratio and center deflections W_C.

	Laminate $[30^o, -30^o]_9$	Laminate $[45^o, -45^o]_9$
h_3/h_1	W_C (mm)	W_C (mm)
0.000	13.1	12.2
0.055	13.23	12.31
0.111	13.35	12.43
0.166	13.45	12.54
0.222	13.56	12.67
0.277	13.66	12.83
0.333	13.77	12.94
0.388	13.88	13.1
0.444	13.98	13.2
0.500	14.05	13.24
0.555	14	13.18
0.611	13.88	13.03
0.666	13.75	12.89
0.722	13.65	12.75
0.777	13.52	12.65
0.833	13.42	12.55
0.888	13.3	12.44
0.944	13.2	12.32
1.000	13.1	12.25

Figure 7 presents the obtained deflections at the centre of the composite plate. As can be noted from the figure that they are symmetrically around the line where h_3/h_1 ratio is equal to 0.5. The ratio 0.5 means the delamination at the midplane, is the highest deflection one. In general, structural stiffness found to be reduced with the location of delamination moves towards the mid-plane. Hence, it leads to the fact that structural instability is more predominant towards the mid-plane of the angle ply anti-symmetric composite laminated structures. From Figure 7, it is observed that the deflection values at angle ply 30^o are the higher than values of deflection at the angle ply 45^o.

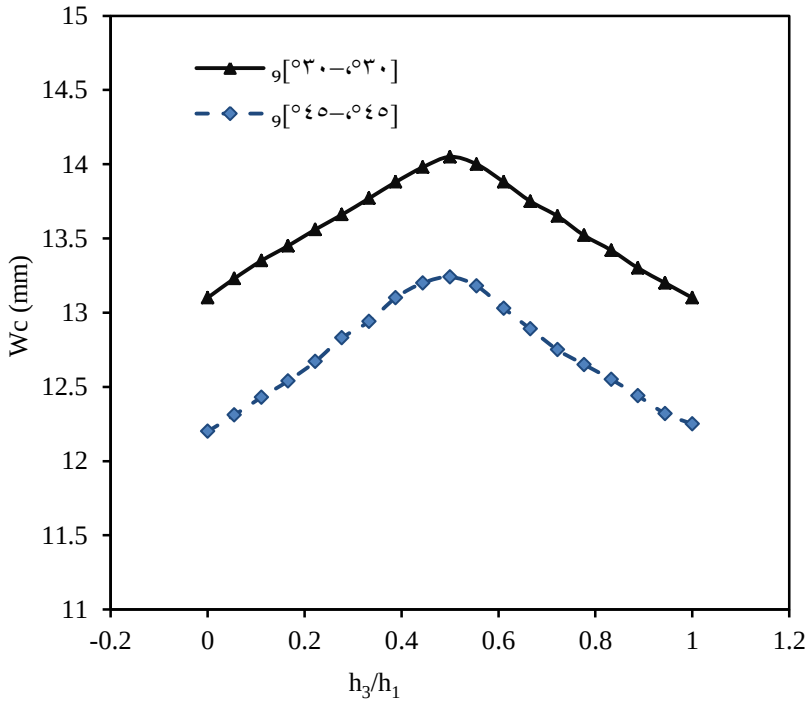

Figure 7 Deflection versus the location of the delamination along the thickness, A_d/A = 0.078

5.4. The effect of delamination area ratio on the deflection at the plate centre:

The example to compute the effect of delamination area to plate laminate area A_d/A ratio, two cases are used first angle ply antisymmetric eighteen layers $[\theta, -\theta]_9$ at $\theta = 45^o$ and the second case cross ply symmetric laminate nine layers $[[0^o, 90^o]_2, 0^o, [90^o, 0^o]_2]$. Figure 8 shows the relationship between the deflection at plate centre (w_c) and A_d/A ratio. It is observed that, the deflection is maximum for delamination area to plate laminate area A_d/A ratio is 0.2 and minimum of delamination area to plate laminate area A_d/A ratio is 0.0. The composite plate in first case is more stiff than second case.

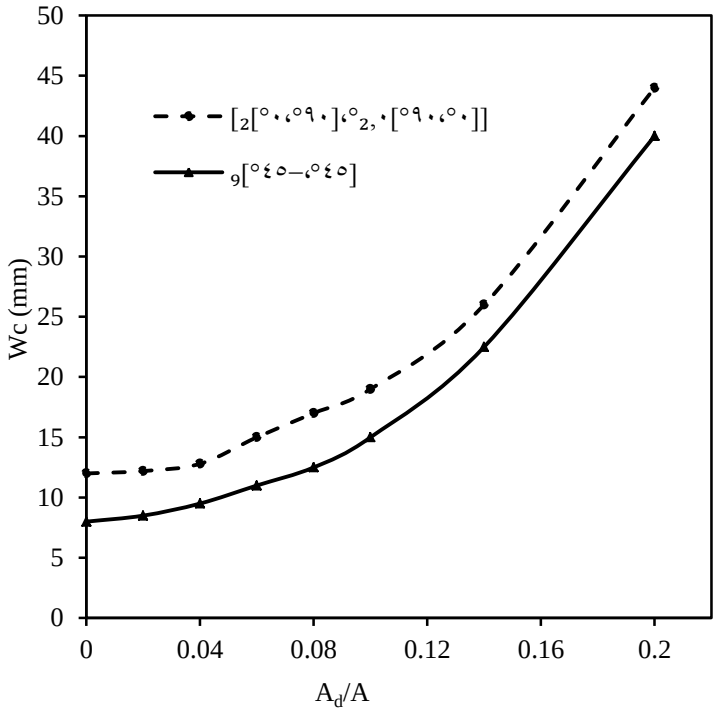

Figure 8 Deflection versus delamination area to plate area ratio

5.5. Comparison of the Failure Criteria:

Before comparison the computer codes were developed to generate the numerical results to study the first ply failure in a laminate for transverse bending by Tsai-Hill criterion, Tsai-Wu criterion and Hoffman criterion. The laminate plate consists of eighteen layers antisymmetric angle-ply $[\theta,-\theta]_9$ subjected under uniform distribution load. Table 5 presents the first-ply failure load effects when the ply angle change from 0^o to 90^o.

The relations between the first-ply failure loads and lamination angle for each criterion are plotted in Figure 9. In general, the results show that the first-ply failure load decreases when the fibres are orientated from 0^o to 45^o and increases when the fibres are orientated from 45^o to 90^o. From the results shown in Figure 9 (antisymmetric laminate), it could be observed that there is no significant difference of the first ply failure load curves between Tsai-Wu, Tsai-Hill and Hoffman criterion, except between angle 0^o until 10^o fibre orientation and between angle 80^o until 90^o fibre orientation. The first ply failure load curves for the 10^o to 80^o orientation are almost similar.

Table 5. First-ply failure load variation with ply angle

θ (deg)	First-ply failure load (N)		
	Tsai-Hill criteria	Tsai-Wu criteria	Hoffman criteria
0	4889.4	5219.2	4326.4
10	1131.6	1123.5	1120.4
15	740.7	710.8	711.2
20	505.5	504.2	504.2
30	480.8	475	477.6

θ (deg)	First-ply failure load (N)		
	Tsai-Hill criteria	Tsai-Wu criteria	Hoffman criteria
45	404.5	402.6	407.5
60	480.1	475	477.2
70	505.5	504.2	504.2
75	740.8	710.6	712
80	1130	1119	1118.7
90	4881.8	5215	4380.6

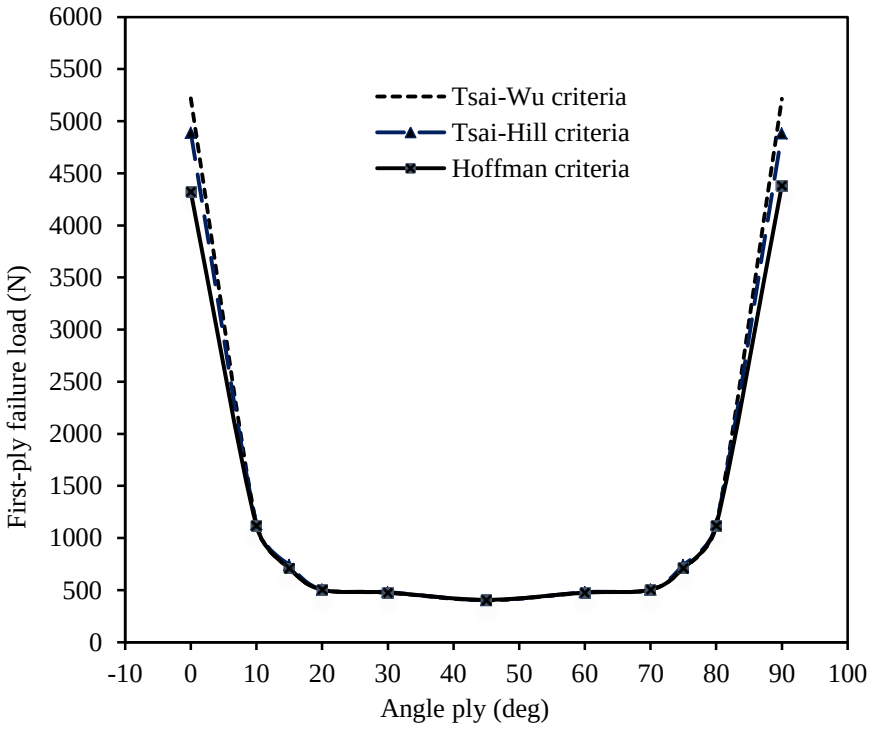

Figure 9 First-ply failure loads versus lamination angle

6. Conclusions:

The present study shows the results of FEM to analyse the deflection at the centre of composite laminate plate with circle delamination, and when compared these results with other methods the deflections agreed very closely.

According to the foregoing analysis the following conclusions are made:

1. The location of delamination along the thickness is effective on the deflection, from the results the maximum deflection at the ratio $h_3/h_1 = 0.5$.
2. Three-plate model is suitable to compute the deflections and stresses of a delaminated composite laminate plate.
3. The deflections of delamination plate are larger than deflections of perfect plate.
4. The delamination area is directly proportional to the deflection at plate centre.
5. According to comparison of the three failure criteria the results of those three criteria are very close to each other. It is clear from those results the three failure criteria are reasonable in analysis of delamination problems.
6. The finite element formulation presented in this paper can be successfully applied to analyse the deflections of delaminated composite plate for any particular laminate configuration

References:

[1] *Gürdal Z, Haftka RT, and Hajela P., Design and optimization of laminated composite materials., Canada: John Wiley & Sons., 1999.*

[2] *Ibrahim MS, Sapuan SM and Faieza AA., "Mechanical and thermal properties of composites from unsaturated polyester filled with oil palm ash," Journal of Mechanical Engineering and Sciences, vol. 2, pp. 133-147, 2012.*

[3] *Reddy A.R., Reddy B.S., Kumar J. S. and Reddy K.V.K., "Bending analysis of laminated composite plates using finite element method," International Journal of Engineering, Science and Technology, vol. 4, no. 2, pp. 177-190, 2012.*

[4] *Jeffrey KJT, Tarlochan F and Rahman MM., "Residual strength of chop strand mats glass fiber/epoxy composite structures: effect of temperature and water absorption," International Journal of Automotive and Mechanical Engineering, vol. 4, pp. 504-519, 2011.*

[5] *Adebisi AA, Maleque MA and Rahman MM., "Metal matrix composite brake rotor: historical development and product life cycle analysis," International Journal of Automotive and Mechanical Engineering,, vol. 4, pp. 471-480, 2011.*

[6] *Remmers JJC and de Borst R., "Delamination buckling of fibre–metal laminates," Composites Science and Technology, vol. 61, p. 2207–2213, 2001.*

[7] *Shan LY., Explicit buckling analysis of fiber-reinforced plastic (FRP) composite structures. Phd Thesis. Department of Civil and Environmental Engineering, Washington State University, USA, 2007.*

[8] *Saponara VL, Muliana H, Haj-Ali R and Kardomateas GA., "Experimental and numerical analysis of delamination growth in double cantilever laminated beams.," Engineering Fracture Mechanics, vol. 687–699, p. 69, 2002.*

[9] *Zou Z, Reid SR, Li S and Soden PD., "Application of a delamination model to laminated composite structures," Composite Structures, vol. 56, p. 375–389, 2002.*

[10] *Elmarakbi AM, Hub N and Fukunaga H., "Finite element simulation of delamination growth in composite materials using LS-DYNA.," Composites Science and Technology, vol. 69, p. 2383–2391, 2009.*

[11] *Wimmer G, Schuecker C and Pettermann HE., "Numerical simulation of delamination in laminated composite components – A combination of a strength criterion and fracture mechanics.," Composites: Part B, vol. 40, p. 158–165, 2009.*

[12] *Gözlüklü B and Coker D., "Modeling of the dynamic delamination of L-shaped unidirectional laminated composites," Composite Structures, vol. 94, p. 1430–1442, 2012.*

[13] *Kameran AJ, Agarwal VC, Pal P. and Srivastava V., "Static and Dynamic Analysis of Composite Laminated Plate," International Journal of Innovative Technology and Exploring Engineering (IJITEE), vol. 3, no. 6, pp. 2278-3075, 2013.*

[14] *Cochelin B, and Poter-Ferry M., "A numerical model for buckling and growth of delaminations in composite laminate," Computer Methods in Applied Mechanics and Engineering, vol. 89, 1991.*

[15] *Chen HP., "Shear Deformation Theory for Compressive Delamination Buckling and Growth," AIAA Journal, vol. 29, no. 5, pp. 813-819, 1991.*

[16] Yahya NA., A study of delamination damage for composite plate in bending. MSc Thesis, Dept. of Solid Mechanics, Beijing University of Aeronautics and Astronautics, China,, 2001.

[17] Reddy JN., "A Simple Higher-Order Theory for Laminated Composite Plates," J. of Applied Mechanics, vol. 51, pp. 745-752, 1984.

[18] Xuanling W. and Yifen Z., " Analysis of Delaminated Composite Plate by Finite Element Method," in Proceeding of 9th Chinese Conference on Composite Material, , pp. 308-313, 1996.